On the evolution of the plant phytochrome chromophore biosynthesis

Federica Frascogna[1], Benjamin Ledermann[1], Jana Hartmann[1], Eugenio Pérez Patallo[1], Fjoralba Zeqiri[2], Eckhard Hofmann[2], Nicole Frankenberg-Dinkel[1*]

[1]*Department of Microbiology, University of Kaiserslautern-Landau, 67663 Kaiserslautern, Germany*

[2]*Protein Crystallography, Faculty of Biology and Biotechnology, Ruhr University Bochum, 44780 Bochum, Germany*

**corresponding author:* nicole.frankenberg@rptu.de*;* phone +49 631 2052353

running head: Phytochrome chromophore biosynthesis in streptophytes

Abstract

Phytochromes are biliprotein photoreceptors present in plants, algae, certain bacteria and fungi. Land plant phytochromes use phytochromobilin (PΦB) as the bilin chromophore. Phytochromes of streptophyte algae, the clade within which land plants evolved, employ phycocyanobilin (PCB), leading to a more blue-shifted absorption spectrum. Both chromophores are synthesized by ferredoxin-dependent bilin reductases (FDBRs) starting from biliverdin IXα (BV). In cyanobacteria and chlorophyta, BV is reduced to PCB by the FDBR phycocyanobilin:ferredoxin oxidoreductase (PcyA), whereas, in land plants, BV is reduced to PΦB by phytochromobilin synthase (HY2). However, phylogenetic studies suggested the absence of any ortholog of PcyA in streptophyte algae and the presence of only PΦB biosynthesis related genes (*HY2*). The HY2 of the early diverging streptophyte alga *Klebsormidium nitens* (formerly *Klebsormidium flaccidum*) was already indirectly indicated to be involved in PCB biosynthesis. Here, we overexpressed and purified a His_6-tagged variant of *K. nitens* HY2 (KflaHY2) in *E. coli*. Employing anaerobic bilin reductase activity assays and coupled phytochrome assembly assays, we were able to confirm the product and to identify intermediates of the reaction. Site-directed mutagenesis revealed two aspartate residues critical for catalysis. While it was not possible to convert KflaHY2 into a PΦB-producing enzyme by simply exchanging the catalytic pair, the biochemical investigation of two additional members of the HY2 lineage enabled us to define two distinct clades, the PCB-HY2 and the PΦB-HY2 clade. Overall, our study gives insight into the evolution of the HY2 lineage of FDBRs.

Introduction

Photosynthesis is arguably one of the most significant biological processes on earth. To harvest light efficiently, photosynthetic organisms possess chlorophyll light-harvesting antennae incorporated in their photosystems. Moreover, some of these organisms are also capable to sense the quality and intensity of the harvested light. To do that, they employ several types of photoreceptors, which are able to absorb photons and to modulate biological activities based on this information (Möglich et al., 2010). Among these photoreceptors, phytochromes can be found in plants, algae, certain bacteria and fungi (Sharrock, 2008). Phytochromes are capable to perceive red and far-red light, by employing open-chain tetrapyrroles as light-sensing chromophores. Although phylogenetically closely related, land plants and streptophyte algae employ different bilins in their phytochromes. Indeed, as far as is known, land plants use the dark green pigment phytochromobilin (PΦB), whereas streptophyte algae employ the cyan pigment phycocyanobilin (PCB) (Wu et al., 1997). The transition from PCB to PΦB as the phytochrome chromophore appears to have coincided with the origin of land plants (Rockwell et al., 2017). The different bound chromophore leads to a blue shift of the photocycles in the phytochromes of streptophyte algae compared to the ones of land plants.

The light-sensing open-chain tetrapyrroles employed in the photoreceptors are all derived from heme. The first step in the biosynthesis of the bilins is the cleavage of the heme macrocycle at the α-methine bridge mediated by heme oxygenases (HOs). This reaction yields the open-chain tetrapyrrole biliverdin IXα (BV), liberating H_2O, CO and Fe^{2+} (Cornejo and Beale, 1988). BV is then subsequently reduced to the specific bilins by a class of enzymes called ferredoxin-dependent bilin reductases (FDBRs) (Figure S1) (Frankenberg et al., 2001; Frankenberg and Lagarias, 2003). In land plants, the enzyme phytochromobilin synthase (HY2) reduces BV in a two-electron reduction at the A-ring 2,3,3^1,3^2-diene system to the dark green pigment PΦB (Figure 1) (Kohchi et al., 2001; McDowell and Lagarias, 2001). In cyanobacteria and chlorophyta, phycocyanobilin:ferredoxin oxidoreductase (PcyA) catalyzes the four-electron reduction of BV to the cyan pigment PCB via the intermediate 18^1,18^2-dihydrobiliverdin (18^1,18^2-DHBV) (Figure 1) (Frankenberg and Lagarias, 2003). Interestingly, the streptophyte alga *Klebsormidium nitens* is known to employ PCB in its phytochromes but only possesses a HY2 homolog (Rockwell and Lagarias, 2017). Using coexpression studies, it was suggested that the HY2 of *K. nitens* (named KflaHY2) is able to synthesize PCB and not PΦB, like its higher plant homolog (Rockwell et al., 2017). Here we provide direct biochemical evidence that recombinant KflaHY2 is able to reduce BV to PCB. In addition, we investigated the reaction in more detail, identifying important catalytic residues. Biochemical characterization of two additional members of the HY2 lineage furthermore enabled us to define two distinct clades.

Overall, our data give more insight into the evolution of this interesting enzyme family and on the evolution of plants phytochromes.

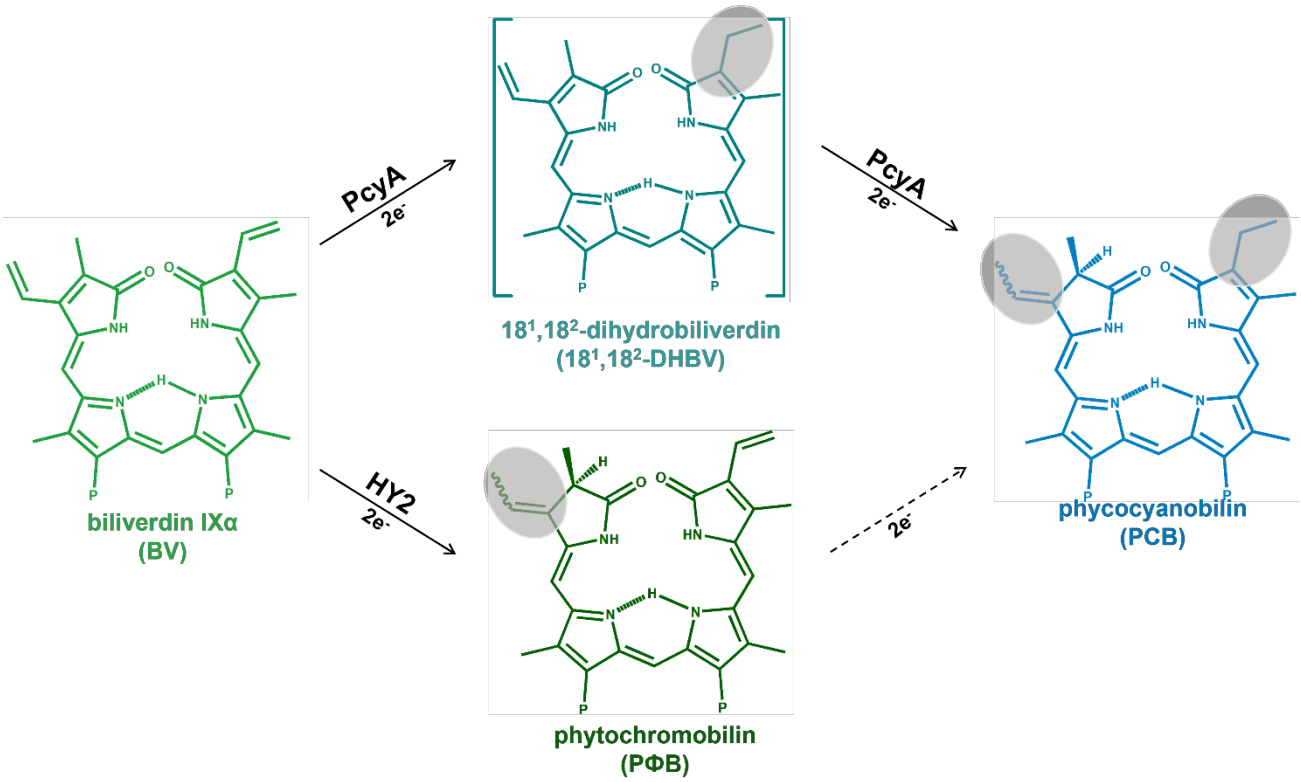

Figure 1 Overview of the reactions catalyzed by the FDBRs HY2 and PcyA. Biliverdin IXα (BV) is the substrate of both FDBRs. "P" indicates the propionate side chains. HY2 catalyzes the two-electron reduction of BV to phytochromobilin (PΦB). PcyA catalyzes the four-electron reduction of BV to phycocyanobilin (PCB) via the intermediate $18^1,18^2$-dihydrobiliverdin (DHBV). Sites of reduction are highlighted in grey. Dashed line represents a possible second pathway to PCB.

93 # Materials and Methods

94 ## Chemicals

95 All chemicals used in this study were ACS grade or better. Most of the components for the
96 anaerobic bilin reductase activity tests were also purchased from Sigma-Aldrich (St. Louis,
97 Missouri, USA), except for biliverdin IXα, which was purchased from Frontier Scientific (Logan,
98 Utah, USA). Ferredoxin (PetF) and FNR (PetH) were recombinantly expressed and purified as
99 described elsewhere (Dammeyer et al., 2008; Busch et al., 2011). HPLC-grade acetone, formic
100 acid and acetonitrile were purchased from VWR Chemicals (Radnor, Pennsylvania, USA).

101 ## Plasmids

102 The plasmid pET28a_*KflaHY2* was gifted by Prof. J. Clark Lagarias (UC Davis, California,
103 USA). Site-directed mutants of KflaHY2 were generated in the pET28a_*KflaHY2* plasmid using
104 the QuikChange® Lightning kit (Agilent, Santa Clara, California, USA) employing primers listed
105 in Table S1. The variant proteins were produced and purified according to the protocol used
106 for KflaHY2 unless stated otherwise. The plasmids pGEX-4T-1_*CepuHY2* and pGEX-4T-
107 1_*NediHY2* were purchased as already cloned by GenScript (Piscataway, New Jersey, USA).
108 The full list of employed constructs can be found in Supplemental Materials (Table S2).

109 ## Production and purification of recombinant proteins

110 For the production of recombinant KflaHY2 and variants, 2 L of LB medium containing the
111 appropriate antibiotics was inoculated 1:100 with an overnight culture of *E. coli* BL21(DE3)
112 carrying the respective plasmids. Cells were grown at 37°C and 100 rpm (Innova® 44, New
113 Brunswick Scientific, Enfield, Connecticut, USA) to an OD_{600} of 0.4-0.6. The temperature was
114 decreased to 17°C and gene expression was induced by the addition of isopropyl-β-D-
115 thiogalactopyranoside (IPTG) to a final concentration of 1 mM (for pET28a_*KflaHY2*) or 0.5
116 mM (for pET28a_*KflaHY2*_N105D, pET28a_*KflaHY2*_D122N, pET28a_*KflaHY2*_D242N,
117 pET28a_*KflaHY2*_N105D_D122N, pET28a_*KflaHY2*_N105D_D242N). The cultures were
118 incubated under shaking for additional 19 h and harvested at 4°C by centrifugation for 10 min
119 at 17000 g (Sorvall™ LYNX™ 6000, Rotor F9). The pellets were resuspended in "binding
120 buffer" (20 mM sodium phosphate pH 7.4; 500 mM NaCl). After the addition of a spatula tip of
121 DNaseI (Applichem, Darmstadt, Germany) and lysozyme (Sigma-Aldrich), the suspension was
122 kept on ice for 30 min. The cells were disrupted by sonication for 5 min (Bandelin Sonopuls
123 HD 2200; tip KE76; 5'' pulses, 10'' pauses; cycle 6/10; ≈ 40% power output) and centrifuged
124 for 45 min at 4°C and 50000 g (Sorvall™ LYNX™ 6000, rotor T29-8). The crude extract was
125 loaded onto a gravity flow column containing 2 mL of TALON® Superflow™ resin (Cytiva,
126 Marlborough, Massachusetts, USA). The column was washed with 10 column volumes (CV)
127 of binding buffer and the elution was performed using 4 CV of "elution buffer" (20 mM sodium

128 phosphate pH 7.4; 500 mM NaCl; 500 mM imidazole). Protein containing fractions were pooled
129 and dialyzed overnight against TES-KCl buffer (25 mM TES/KOH pH 7.5; 100 mM KCl; 10%
130 glycerol).
131 Production of NediHY2 and CepuHY2 was carried out adding minor adjustments to the above-
132 mentioned protocol. During expression, after an OD_{600} of 0.4-0.6 was reached, the main culture
133 was subjected to a cold shock at 4°C for 1h, before inducing with 0.5 mM IPTG. The cultures
134 were incubated under shaking at 17°C for additional 19 h before harvesting. The pellets were
135 resuspended in "lysis buffer" (50 mM Tris-HCl pH 7.5; 150 mM NaCl) and a spatula tip of
136 DNAse was added to the resuspension alongside 1 mM PMSF. After homogenizing the
137 resuspension with a douncer, lysis was carried out using a Microfluidics™ M-110L
138 microfluidizer (3-5 cycles, 800-1000 bar). The disrupted cells were subjected to
139 ultracentrifugation at 4°C and 235000 g for 1h (Beckman Optima™ L-80 XP, rotor Ti45). The
140 resulting supernatant was loaded onto an Äkta purifier system (GE HealthCare, Chicago,
141 Illinois, USA) equipped with a 25 mL self-packed 20/26 GSTrap column (GE HealthCare). A
142 linear gradient containing 50 mM reduced glutathione in "lysis buffer" was used for elution.
143 Protein containing fractions were pooled and buffer exchange was carried out using a PD-10
144 column (GE Healthcare) using TES-KCl buffer (25 mM TES/KOH pH 7.5; 100 mM KCl; 10%
145 glycerol). The fusion protein was cleaved using Thrombin (from bovine plasma, 50 NIH
146 units/mg dry wt) following the manufacturer's instructions (Sigma-Aldrich). The following day,
147 after concentrating the protein (Amicon® Ultra MWCO 30 kDa, Merck, Darmstadt, Germany),
148 a second GST-tag purification was performed and the peak fractions were pooled and
149 concentrated (Amicon® Ultra MWCO 10 kDa, Merck).
150 GST-tagged PcyA and GST-tagged mHY2 were produced and purified as described previously
151 (Kohchi et al., 2001; Frankenberg and Lagarias, 2003). Apo-Cph1 and apo-BphP were
152 produced as described elsewhere (Tasler et al., 2005a; Fiege and Frankenberg-Dinkel, 2020).
153 The concentration of the purified proteins was determined based on the absorbance at 280 nm.
154 Extinction coefficients were calculated as described by Gill and von Hippel (Gill and von Hippel,
155 1989).

156 Anaerobic bilin reductase assay

157 The anaerobic bilin reductase activity assays were performed as described previously with
158 minor modifications (Ledermann et al., 2016). In this study, recombinant ferredoxin PetF from
159 the cyanophage P-SSM2 was used as the electron donor in a final concentration of 1 µM. PetF
160 was reduced using recombinant Ferredoxin-$NADP^+$ reductase (FNR) from *Synechococcus* sp.
161 PCC7002, PetH, at a final concentration of 0.01 µM (Busch et al., 2011). The reaction was
162 started by the addition of a NADPH regenerating system consisting of 65 mM glucose-6-
163 phosphate, 8.2 µM NADP+ and 11 U/ml glucose-6-phosphate dehydrogenase. For the assays
164 employing defined electron equivalents, the NADPH regenerating system was replaced with a

165 NADPH solution of a specific concentration. The photometric measurements were carried out
166 using an Agilent 8453 spectrophotometer. The reaction was stopped by the dilution 1:10 in ice
167 cold 0.1% TFA. Products were isolated via solid phase extraction using Sep-Pak® C18 Plus
168 Light cartridges (Waters, Milford, Massachusetts, USA) and freeze-dried using an Alpha 2-4
169 LSC plus lyophilizer (Martin Christ GmbH, Osterode, Germany).

170 HPLC analyses

171 The products of the anaerobic bilin reductase assays were analyzed using an Agilent 1100
172 series chromatograph equipped with a Luna® 5µm reversed phase C18-column (Phenomenex,
173 Torrance, California, USA) and a diode-array detector. The mobile phase consisted of 50%
174 (v/v) acetone and 50% (v/v) 20 mM formic acid at a flow rate of 0.6 mL/min. Reaction products
175 were identified by comparison of the retention time with known standards as well as whole
176 spectrum analysis of the elution peaks. Products of interest were collected directly at the outlet
177 of the UV-Vis detector, frozen at -80°C and freeze-dried.

178 Coupled phytochrome assembly assays

179 *In vitro* chromophore assembly of the apo-phytochromes Cph1 and BphP with different bilins
180 was carried out using the lysate of a pET_*cph1* or a pASK_*bphP* overexpression after
181 centrifugation and filtration. The assembly was tested employing 50 µL lysate incubated either
182 with 40 µM standard bilin or with 4 µL of bilin solutions of unknown concentration for 30 min at
183 room temperature, in the dark. Afterwards, the volume was adjusted to 500 µL with PBS.
184 Absorbance spectra were recorded after incubation for 3 min with red light (636 nm – Pr
185 spectrum) and after incubation for 3 min with far red light (730 nm for Cph1; 750 nm for BphP
186 – Pfr spectrum). Difference spectra were calculated by the subtraction of the Pfr from the Pr
187 spectrum.

188 Phytofluor analyses

189 Phytofluor formation was evaluated via fluorescence measurements (Murphy and Lagarias,
190 1997). Briefly, 50 µL lysate of a pET_*cph1* or a pASK_*bphP* overexpression, after
191 centrifugation and filtration, was incubated with 4 µL of the KflaHY2_N105D reaction product,
192 for 30 min, at room temperature, in the dark. Afterwards, the volume was adjusted to 500 µL
193 with PBS. Fluorescence spectra were recorded using a JASCO FP-8300 spectrofluorometer
194 (JASCO, Tokyo, Japan).

195 Protein structure prediction and analyses

196 KflaHY2 structure prediction was performed using AlphaFold via ColabFold (Jumper et al.,
197 2021; Mirdita et al., 2022). Parameters set for the AlphaFold algorithm were the following:
198 msa_mode: MMseqs2 (UniRef + Environmental), pair_mode: unpaired + paired, model_type:

199 auto, num_recycles: 3. The obtained structure (pLDDT = 89.1) was compared to other
200 crystalized FDBRs using the molecular visualization software PyMOL (DeLano, 2020).

201 Phylogenetic analysis

202 A multiple sequence alignment (MSA) of ferredoxin-dependent bilin reductases was
203 constructed using ClustalW (https://www.ebi.ac.uk/Tools/msa/clustalo/). The obtained MSA
204 was processed employing PhyML 3.0 (http://www.atgc-montpellier.fr/phyml/) (Guindon et al.,
205 2010) with the following command line: -D aa -B 100 -M WAG -V e -C 4 -F m -A e -O tlr.
206 Statistical support was assessed using the transfer bootstrap expectation (TBE) in BOOSTER
207 (https://booster.pasteur.fr/) (Lemoine et al., 2018). Tree was displayed and modified using
208 iTOL (https://itol.embl.de/) (Letunic and Bork, 2021).

Results

KflaHY2 catalyzes the reduction of BV to PCB

It has been known for quite some time that the phytochromes of streptophyte algae use PCB as their chromophore instead of the PΦB found in land plants phytochrome (Wu et al., 1997; Rockwell et al., 2017). Nevertheless, the streptophyte alga *K. nitens* possesses an FDBR homolog to land plant HY2 which was indirectly suggested to be producing PCB (Rockwell et al., 2017). In order to biochemically investigate this, the reductase was recombinantly overproduced in *E. coli* and purified to test its activity (Figure 2A).

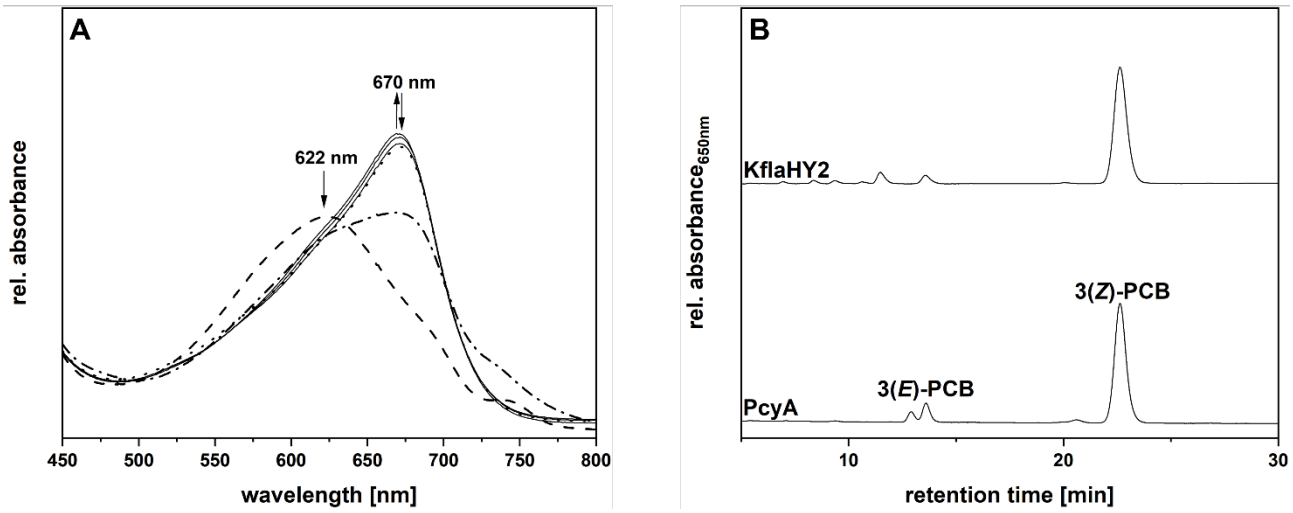

Figure 2 Activity assay of recombinant KflaHY2 employing BV as the substrate and characterization of reaction products. A. Time-resolved UV-Vis spectra of an anaerobic bilin reductase activity of recombinant KflaHY2 employing BV as the substrate. Total reaction time was 5 min and spectra were recorded every 30s. The course of the spectra is marked by arrows. For reasons of clarity, only relevant spectra are shown. The dashed spectrum was acquired without starting the reaction. The dotted-dashed spectrum represents the first acquired after starting the reaction. The dotted curve represents the end spectrum. B. HPLC analyses of the reaction products of KflaHY2 with BV as substrate. The products were analyzed using a reversed-phase 5 µm C18 Luna column (Phenomenex) as stationary phase. The mobile phase consisted of 50% (v/v) acetone and 50% (v/v) 20 mM formic acid flowing at 0.6 mL/min. Products of an anaerobic turnover of BV to PCB mediated by PcyA served as standards. Absorbance was continuously recorded at 650 nm.

Interestingly, the reductase and the substrate BV formed an intense turquoise colored complex with an absorbance maximum at 622 nm, suggesting that the reductase was folded correctly and was able to bind BV (Figure 2A). The presence of a shoulder at ~ 750 nm indicates the presence of BV in its protonated form (Frankenberg and Lagarias, 2003; Tu et al., 2004). After the reaction was started, the absorbance decreased instantly. Moreover, a rapid formation of a product with an absorbance maximum at 670 nm, which can be linked to the formation of PCB, was observed. Subsequent HPLC analyses, employing the reaction products of PcyA as standards, revealed that KflaHY2 forms 3(*Z*)-PCB as the main reaction product (Figure 2B).

KflaHY2 reaction can proceed via two intermediates

As the KflaHY2 reaction product PCB is a tetrahydro-BV, the reaction should proceed via a two-electron reduced intermediate: either the A-ring reduced PΦB, or the D-ring reduced $18^1,18^2$-DHBV. Intermediates of the reaction were isolated using the products of an anaerobic bilin reductase activity assay conducted with one electron equivalent of NADPH. HPLC analyses of the products showed that KflaHY2 forms two intermediates (Figure 3 – marked as "Inter 1" and "Inter 2").

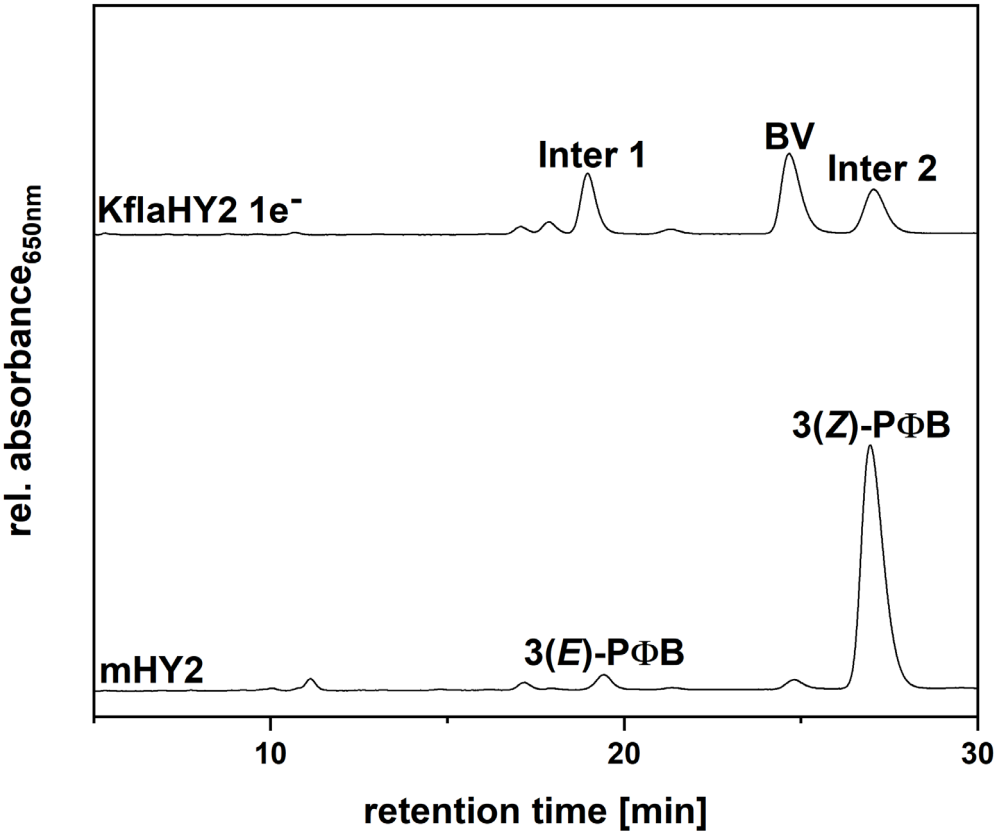

Figure 3 HPLC analyses of the reaction products of an anaerobic activity assay employing equimolar amounts of KflaHY2 and BV with one electron equivalent of NADPH. Products were resolved using a reversed-phase 5 µm C18 Luna column (Phenomenex) as stationary phase and a mixture of 50% (v/v) acetone and 50% (v/v) 20 mM formic acid as mobile phase at 0.6 mL/min. The products of an anaerobic turnover of BV to PΦB mediated by HY2 derived from *A. thaliana* were used as standards. Absorbance was continuously recorded at 650 nm.

The intermediates possessed the same retention times as the products 3(*E*)-PΦB (~ 19 min) and 3(*Z*)-PΦB (~ 27 min) of the recombinant reductase HY2 from *A. thaliana* (mHY2). However, $18^1,18^2$-DHBV, the intermediate of the cyanobacterial PcyA reaction towards PCB, and 3(*E*)-PΦB are roughly characterized by the same retention time. Therefore, "Inter 1" could have been either of the two (Frankenberg and Lagarias, 2003).

The intermediates formed by KflaHY2 are $18^1,18^2$-DHBV and 3(*Z*)-PΦB

To confirm the nature of the intermediates identified by HPLC analyses, coupled phytochrome assembly assays of the isolated intermediates with the apo-phytochromes Cph1 from

260 *Synechocystis* sp. PCC 6803 and BphP from *Pseudomonas aeruginosa* were conducted
261 (Figure 4A). Cph1 finds its natural chromophore in PCB, while BphP uses BV. However,
262 phytochromes are also able to accommodate different bilins as long as they possess the same
263 A-ring configuration as the natural chromophore. Thus, Cph1 is able to bind bilins possessing
264 an ethylidene group at the A-ring, whereas BphP only binds bilins with an A-ring endo-vinyl
265 group (Li and Lagarias, 1992; Tasler et al., 2005b). Apo-Cph1 incubated with "Inter 1" did not
266 produce a photoactive adduct since no characteristic difference spectrum was obtained,
267 indicating the lack of the ethylidene group at the A-ring C3 side chain (Figure 4A – dashed line)
268 (Xu et al., 2019). This led to the conclusion that "Inter 1" could not be 3(*E*)-PΦB. Incubation of
269 apo-Cph1 with "Inter 2" (Figure 4A – dotted line) led to a difference spectrum like it was
270 obtained for the incubation of Cph1 with 3(*Z*)-PΦB (Figure 4A – solid line). These results, as
271 well as the results of the HPLC analyses (Figure 3), prove that "Inter 2" is 3(*Z*)-PΦB.
272

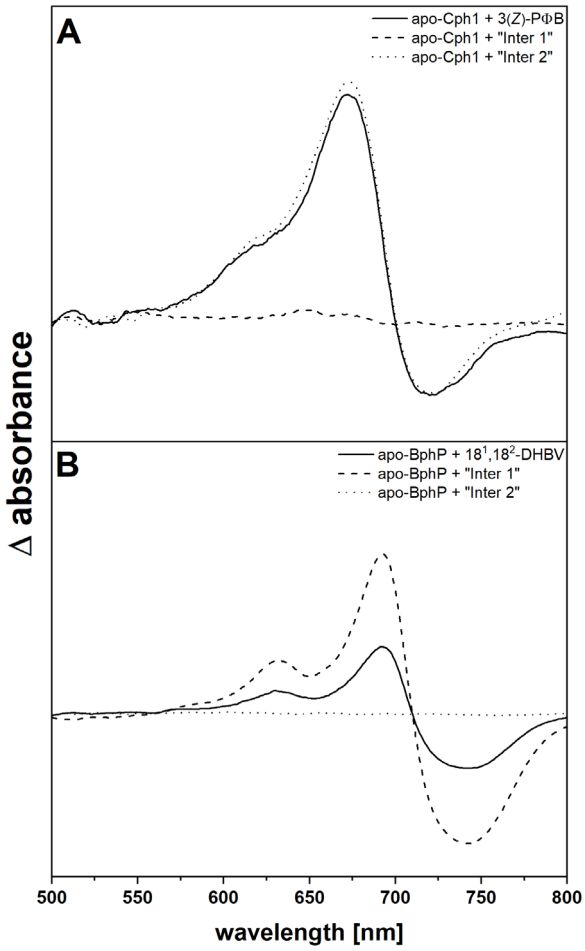

273

274 **Figure 4** Red/far-red light induced difference spectra of coupled phytochrome assembly assays employing the
275 intermediates of the KflaHY2 reaction. Absorbance spectra were recorded after incubation for 3 min with red light
276 (636 nm – Pfr spectrum) and after incubation for 3 min with far red light (730 nm for Cph1; 750 nm for BphP – Pr
277 spectrum). Difference spectra were calculated by the subtraction of the Pfr from the Pr spectrum. All calculated
278 difference spectra were smoothed applying a 20 pt. Savitzky-Golay filter. A. Coupled phytochrome assembly assays
279 employing apo-Cph1 and "Inter 1" (dashed line); apo-Cph1 and "Inter 2" (dotted line); apo-Cph1 and 3(*Z*)-PΦB
280 (solid line) B. Coupled phytochrome assembly assay employing apo-BphP and "Inter 1" (dashed line); apo-BphP
281 and "Inter 2" (dotted line); apo-BphP and 18^1,18^2-DHBV (solid line).

282 On the other hand, “Inter 2” failed to form a photoactive adduct with apo-BphP (Figure 4B –
283 dotted line), whereas, “Inter 1” formed a photoactive adduct with apo-BphP with a difference
284 spectrum (Figure 4B – dashed line) similar to the difference spectrum obtained by the
285 incubation of BphP with 18^1,18^2-DHBV (Figure 4B – solid line). This revealed that “Inter 1” is
286 indeed 18^1,18^2-DHBV.
287 To clarify whether the intermediates are only artifacts of the *in vitro* assay or if they are actually
288 suitable in KflaHY2-catalyzed BV reduction, both compounds were used as substrates for
289 KflaHY2 in anaerobic bilin reductase activity assays. Subsequent HPLC analyses revealed
290 that both intermediates are transformed to mostly 3(*Z*)-PCB (Figure 5).
291

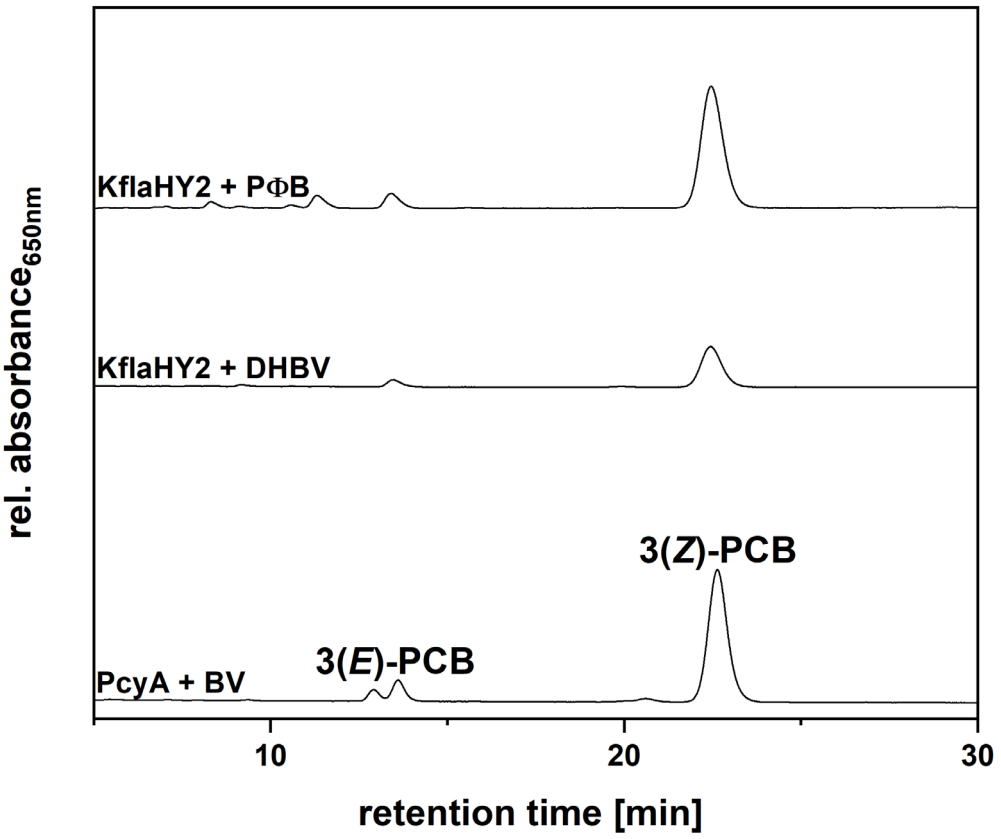

292

293 **Figure 5** HPLC analyses of the reaction products of activity tests employing 3(*Z*)-PΦB and 18^1,18^2-DHBV as
294 substrates for KflaHY2. Products were analyzed using a 5 µm reversed-phase C18 Luna column (Phenomenex) as
295 stationary phase. The mobile phase consisted of 50% (v/v) acetone and 50% (v/v) 20 mM formic acid flowing at 0.6
296 mL/min. Reaction products of a PcyA mediated reduction of BV to PCB were used as standards. Absorbance was
297 continuously recorded at 650 nm.

298 Asp^{122} and Asp^{242} are essential for the catalytic activity

299 In order to gain further insight on the unexpected behavior of KflaHY2 and to learn about the
300 evolution of HY2, an amino acid sequence alignment employing different FDBRs was
301 constructed (Figure S2). Three residues caught our attention: Asn^{105}, Asp^{122} and Asp^{242}.
302 KflaHY2 Asn^{105} represents the homolog to *Synechocystis sp.* PCC 6803 PcyA His^{88}, which was
303 proven to be involved in protonation and substrate positioning in the active site (Hagiwara et
304 al., 2010). The substitution of the His to an Asn is not unusual since it can also be found in

305 other FDBRs like PebA, PebB and PebS. On the other hand, land plants HY2s show an Asp
306 in the corresponding position which was also proven to be essential for substrate positioning
307 in *Arabidopsis thaliana* HY2 and involved in catalysis in *Solanum lycopersicum* HY2 (SlHY2)
308 (Tu et al., 2008; Sugishima et al., 2020). KflaHY2 Asp^{122} finds a homolog in all the FDBRs
309 except for the ones from land plants. In PcyA and PebS, it is located in the central β-sheet of
310 the binding pocket and was shown to be the initial proton donor (Hagiwara et al., 2006; Busch
311 et al., 2011). Finally, Asp^{242} finds a homolog in Asp^{256} of *A. thaliana* HY2, Asp^{256} of *S.*
312 *lycopersicum* HY2 (SlHY2), Asp^{206} of PebS and Asp^{219} of *Guillardia theta* PEBB. All of these
313 Asp residues were shown to be involved in the reduction of the A-ring $2,3,3^1,3^2$-diene system
314 (Tu et al., 2008; Busch et al., 2011; Sommerkamp et al., 2019; Sugishima et al., 2020). On the
315 basis of these considerations, site-directed mutagenesis was performed. To investigate the
316 influence of ionization on catalysis, Asp^{122} and Asp^{242} were replaced by asparagine residues
317 whereas Asn^{105} was replaced by an aspartate residue. Moreover, two double variants were
318 generated. In particular, one was constructed for KflaHY2 to resemble a plant HY2, the other
319 to prove the presence of two Asp residues is enough for reducing BV to PCB. The activity of
320 the purified variant enzymes was investigated *in vitro* via FDBR assays and subsequent HPLC
321 analyses (Figure 6).

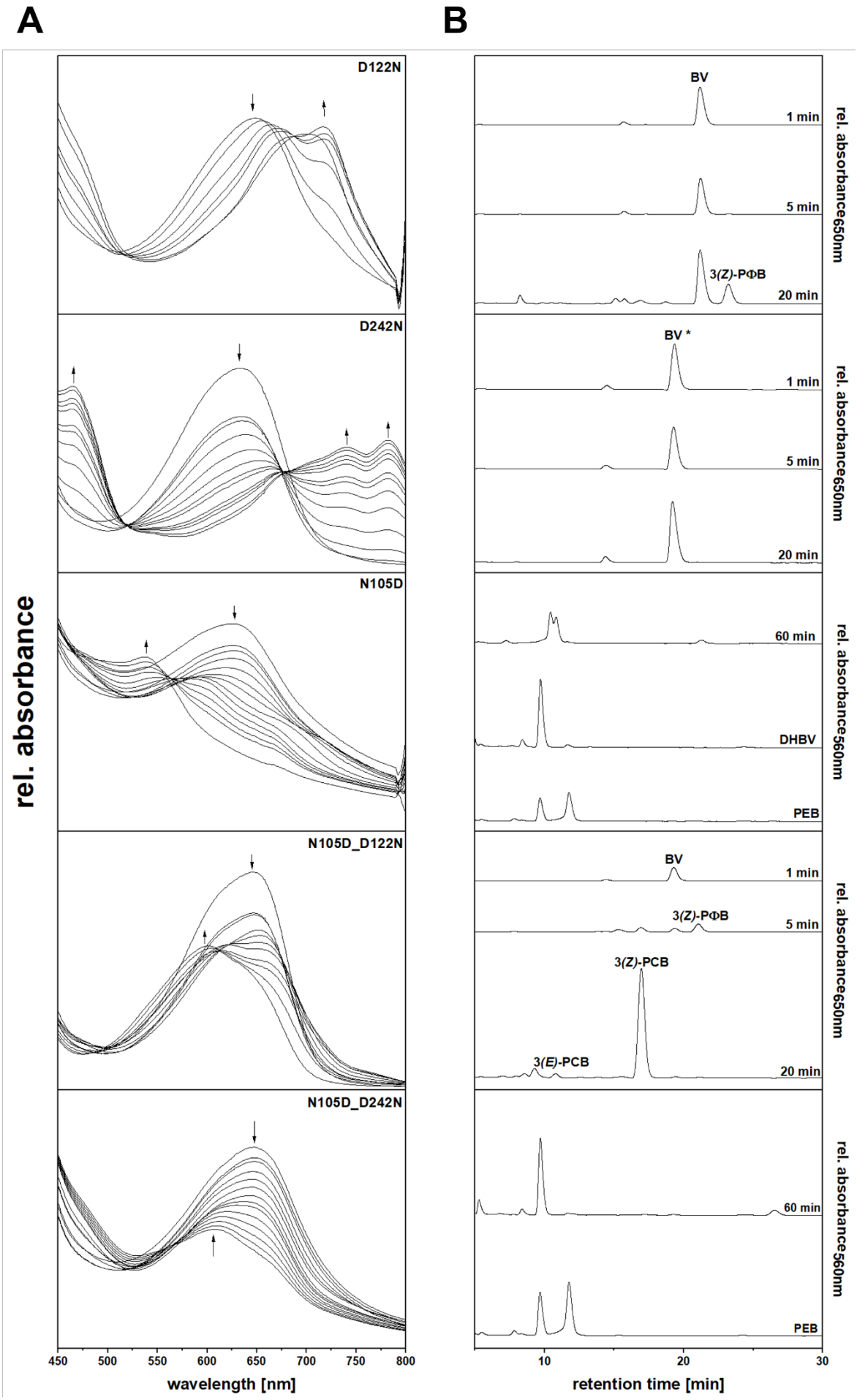
A
B
D122N
D242N
N105D
N105D_D122N
N105D_D242N
rel. absorbance
450
500
550
600
650
700
750
800
wavelength [nm]
BV
1 min
5 min
3(Z)-PΦB
20 min
BV *
60 min
DHBV
PEB
3(Z)-PCB
3(E)-PCB
rel. absorbance650nm
rel. absorbance560nm
10
20
30
retention time [min]

Figure 6 Activity assay and characterization of reaction products of recombinant KflaHY2 variants. A. UV-Vis spectra of the anaerobic FDBR Assay performed using KflaHY2 variants and BV as the substrate. Total reaction time was 20 minutes for KflaHY2_D122N, KflaHY2_D242N, KflaHY2_N105D_D122N and 60 min for KflaHY2_N105D, KflaHY2_N105D_D242N. Spectra were recorded every 30 seconds. For reasons of clarity, only relevant spectra are shown. The arrow indicates the course of absorbance during the reaction. B. HPLC elution profiles of the reaction products of KflaHY2 variants. The stationary phase consisted in a Luna 5µm reversed phase C18 column (Phenomenex). The mobile phase consisted of a mixture of 50% (v/v) acetone and 50% (v/v) 20mM formic acid flowing at 0.6 mL/min. Absorbance was continuously recorded at 560 or 650 nm. BV shows change in the retention time due to substitution of the mobile phase between the different HPLC measurements (*).

The D122N variant was able to bind BV and use it as a substrate, since the formation of a peak at ~ 720 nm was observed (Figure 6A – D122N). Intermediates were isolated from the reaction mix at certain time points and analyzed via HPLC. Time-course HPLC analyses revealed the formation of small amounts of 3(*Z*)-PΦB after 20 min from the start of the reaction (Figure 6B – D122N). This variant partially retains the capability to reduce the BV A-ring but is completely unable to reduce the D-ring, thus proving the importance of D122 for D-ring reduction.

The D242N variant still retained the ability to bind BV but failed in its reduction. The increase of the absorption at ~ 460, ~ 740 and ~ 790 nm suggested the formation of the radical BVH• (Figure 6A – D242N) (Tu et al., 2004; Tu et al., 2008; Busch et al., 2011). The HPLC elution profiles were compatible with BV, therefore confirming the inactivity (Figure 6B – D242N). This result is consistent with what was found for mHY2_D256N and SlHY2_D263N indicating the importance of this residue for BV protonation (Tu et al., 2008; Sugishima et al., 2020).

The N105D variant showed an unexpected behavior. The assay was initially performed for 20 min but strangely revealed the formation of a violet-colored product with a peak ~ 570 nm, suggesting production of either phycoerythrobilin (PEB) or 15,16-dihydrobiliverdin (15,16-DHBV) (data not shown). In order to potentially accumulate more of this violet compound, we decided to let the reaction run for a longer time, 60 min. This second assay showed the formation of a final product with an absorbance peak at ~ 540 nm (Figure 6A – N105D). Time-based HPLC analyses revealed that the bilin produced after 5 min from the start of the reaction was indeed PCB, whereas a pattern compatible with the unidentified compound and mostly 3(*Z*)-PCB was obtained for the 20 min product (data not shown). As for the final 60 min product, HPLC analysis revealed a double peak with the retention time of 10.5 and 10.8 min, not matching the retention time of any known bilin and therefore leading to uncertainty (Figure 6B – N105D). To identify the unknown bilin, its integration in the phytochromes Cph1 and BphP was evaluated. PEB and 15,16-DHBV lack the C15-16 double bond required for the photoconversion of the phytochrome between the two isoforms. Therefore, phytochromes binding bilins lacking the C15-16 double bond are locked in the red-light absorbing form. In this condition, there is no complete de-excitation of the bilin, leading to the formation of a fluorescent product named phytofluor (Murphy and Lagarias, 1997). The bilin product isolated from the reaction catalyzed by KflaHY2_N105D was then incubated in parallel with the two apo-phytochromes and fluorescence was measured. The formation of a characteristic

365 phytofluor was only observed for the incubation with apo-Cph1, thus suggesting the product is
366 PEB (Figure 7).

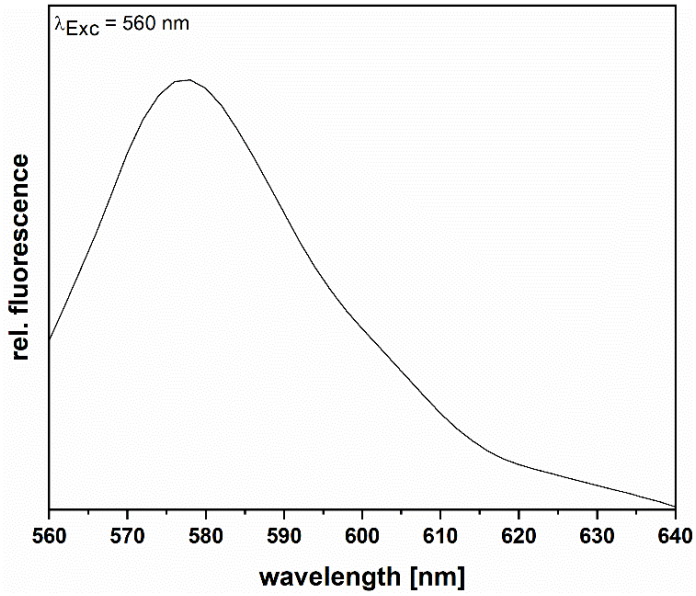

367

368 **Figure 7** Fluorescence emission spectrum of the apo-Cph1-KflaHY2_N105D reaction product adduct. The isolated
369 bilin produced by KflaHY2_N105D was incubated for 30 min in the dark with the lysate of a pET_*cph1*
370 overproduction. Fluorescence emission was recorded after excitation at 560 nm.
371
372 The double variant N105D_D122N, constructed to mimic a plant HY2, surprisingly retained the
373 native activity, revealing the conversion of BV to PCB instead of the hypothesized $2e^-$ reduction
374 to PΦB (Figure 7 – N105D_D122N). This result led to the hypothesis that the presence of two
375 aspartate residues in the active site, even if in different position than in the native enzyme, is
376 enough for the reduction of BV to PCB. To further investigate it, the double variant
377 N105D_D242N was also generated. Interestingly, performing the assay for 60 min revealed
378 the formation of a pink product with an absorbance at ~ 600 nm (Figure 6A – N105D_D242N).
379 Via HPLC analysis, the final product was identified to be 3(*E*)-PEB (Figure 6B –
380 N105D_D242N), thus showing a different activity than expected.
381

382 *Netrium digitus* HY2 is also a PCB synthesizing enzyme

383 Since our attempt to convert the *K. nitens* HY2 enzyme into a plant type HY2 with PΦB
384 biosynthetic activity failed, we decided to go back to a phylogenetic tree of the HY2 lineage
385 (Figure 8) to select sequences for biochemical assays and identify where the change of activity
386 happened.

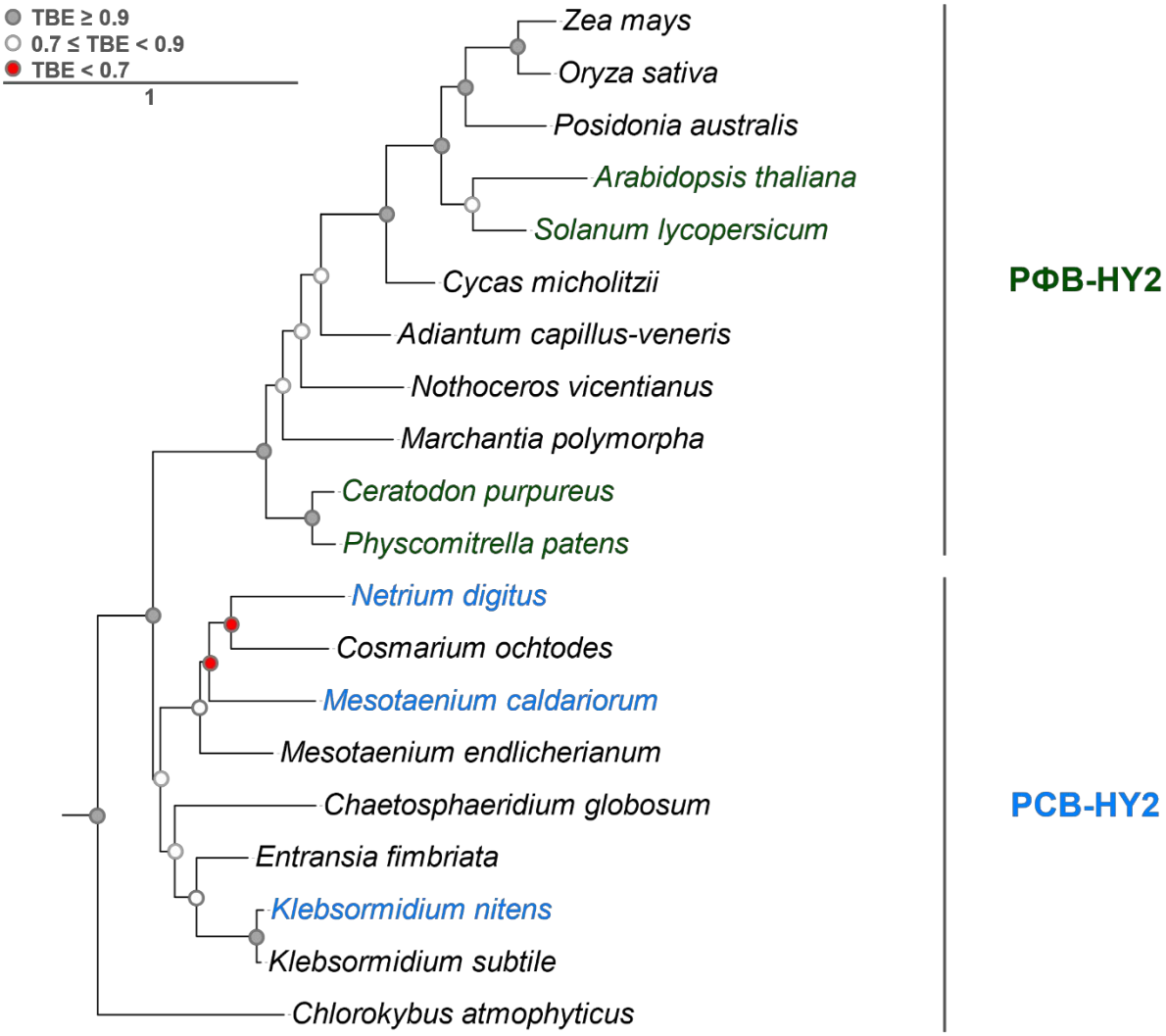

Figure 8 Phylogenetic analysis of HY2 lineage of FDBRs. The maximum-likelihood tree was inferred using PhyML (Guindon et al., 2010). Transfer bootstrap expectation (TBE) was used for support. The represented tree is an excerpt of a full tree including members of all the FDBRs lineages (employed sequences in Supp. DataFile1). Accession numbers of the shown sequences are available in Supplemental material (Table S3). Labels indicate HY2-belonging organism. The color of the label represents the produced bilin (cyan for PCB, dark green for PΦB). Only HY2 with experimentally proven activity are colored. Circles at nodes indicate TBE (grey, TBE ≥ 0.9; white, 0.7 ≤ TBE < 0.9; red, TBE < 0.7).

The *Physcomitrella patens* HY2 has been studied previously and was shown to convert BV to PΦB (Chen et al., 2012) (Shih-Long Tu, Academia Sinica, Taiwan, personal communication). *Mesotaenium caldariorum* was previously shown to synthesize its PCB phytochrome chromophore via PΦB using cell free extracts (Wu et al., 1997). Therefore, we decided to have a look at the HY2s from *Ceratodon purpureus* and *Netrium digitus* (NediHY2). Unfortunately, both recombinant proteins were prone to aggregation but we managed to obtain enough catalytic activity for product identification. While the HY2 of *C. purpureus* confirmed previous indirect evidence and synthesized PΦB from BV (Lamparter et al., 1995) (data not shown),

405 NediHY2 was shown to produce PCB in a coupled phytochrome assay using apo-Cph1 (Figure
406 9).

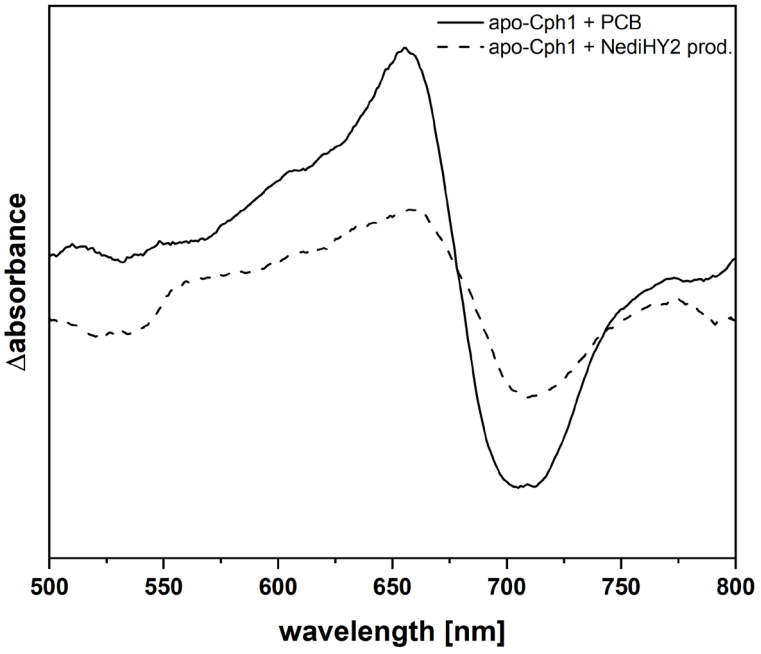

407

408 **Figure 9** Red/far-red light induced difference spectra of coupled phytochrome assembly assays employing PCB
409 and the product of the NediHY2 reaction. Absorbance spectra were recorded after incubation for 3 min with red
410 light (636 nm – Pfr spectrum) and after incubation for 3 min with far red light (730 nm – Pr spectrum). Difference
411 spectra were calculated by the subtraction of the Pfr from the Pr spectrum. The apo-Cph1 + PCB difference
412 spectrum (solid line) was smoothed applying a 20 pt. Savitzy-Golay filter. The apo-Cph1 + NediHY2 prod. difference
413 spectrum (dashed line) was smoothed applying a 80 pt. Savitzky-Golay filter.
414

415 Based on these data and the phylogenetic tree of the HY2 lineage of FDBRs, we can conclude
416 that the switch of activity from a PCB-producing to a PΦB-producing HY2 enzyme happened
417 within the streptophyte HY2 lineage, likely between *Netrium digitus* and *Physcomitrella patens*.

418 *Discussion*

419 Over two decades ago, the last of the classic photomorphogenetic mutants of *Arabidopsis*
420 *thaliana*, *hy2*, was cloned (Kohchi et al., 2001). *HY2* encodes phytochromobilin synthase, the
421 first member of the ferredoxin-dependent bilin reductase family, catalyzing the last step in plant
422 phytochrome chromophore biosynthesis. Subsequently, multiple members of the FDBR family
423 were identified in cyanobacteria, red algae, mosses and cryptophytes (Frankenberg et al.,
424 2001; Chen et al., 2012; Overkamp et al., 2014; Rockwell and Lagarias, 2017). All share the
425 same overall fold consisting of an α-/β-/α-sandwich which harbours the active side on top of
426 the central β-sheet. With the number of recombinant FDBRs biochemically characterized, it
427 became clear that it is not always possible to predict the catalytic activity solely based on an
428 amino acid sequence alignment (Dammeyer et al., 2008; Ledermann et al., 2018). One reason
429 is attributable to the substrate binding mode. Indeed, the crystal structure of both PebB and
430 HY2 revealed a *ZZZssa* flipped binding mode of the linear tetrapyrrole substrate
431 (Sommerkamp et al., 2019; Sugishima et al., 2020). Both enzymes have furthermore in

432 common that they reduce the A-ring 2,3,3^1,3^2-diene system of the substrate. Their relatedness
433 is phylogenetically supported as HY2 is part of the PebB lineage of FDBRs (Rockwell and
434 Lagarias, 2017). That said, it was rather unexpected to find out that streptophyte algae all bare
435 HY2 homologs, although their phytochromes employ a PCB chromophore (Wu et al., 1997;
436 McDowell and Lagarias, 2001; Rockwell et al., 2017). These bilins are characterized by
437 different spectral properties: while PCB absorbs orange and red light (λ_{PCB} = ~ 620 - 670 nm),
438 PΦB absorbs far-red light ($\lambda_{P\Phi B}$ = ~ 660 - 685 nm). In the present study, we confirmed that the
439 HY2 of *Klebsormidium nitens* is indeed a functional FDBR, which, in contrast to the
440 phylogenetic classification as a HY2, possesses a PcyA-like activity, catalyzing the reduction
441 of BV to PCB. Furthermore, we identified 18^1,18^2-DHBV and 3(*Z*)-PΦB as intermediates
442 occurring under the chosen assay conditions. These results were somehow unexpected, as
443 they lead to the conclusion that KflaHY2 can mediate the reduction of BV to PCB employing
444 two different reaction routes (Figure 1). However, the formation of 3(*Z*)-PΦB as an intermediate
445 during PCB biosynthesis is tying well with previous phytochrome studies in the
446 Zygnematophycea *Mesotaenium caldariorum*, an organism that also possesses a HY2 (Figure
447 9) (Wu et al., 1997). Taking this into consideration, we propose that PΦB is the real
448 intermediate in the KflaHY2 catalyzed conversion of BV to PCB and the formation of the
449 18^1,18^2-DHBV intermediate is rather an experimental artefact. Here it is possible that, during
450 *in vitro* enzyme assays, the substrate BV is forced into the active site in two orientations leading
451 to the two observed isomers. *In vivo*, the substrate might be directly channeled from the
452 preceding enzyme, heme oxygenase. A similar scenario has been described for certain heme
453 oxygenases from pathogenic bacteria where the orientation of the substrate dictates the
454 product formed (Caignan et al., 2002). This is further supported by a structural model of
455 KflaHY2 obtained using AlphaFold (Jumper et al., 2021) and two structural alignments using
456 PyMOL: one with the crystal structure of the HY2 of *Solanum lycopersicum*, with which KflaHY2
457 shares high sequence homology, the second with the crystal structure of PcyA of
458 *Synechocystis* sp. PCC 6803 (SynPcyA), catalyzing BV to PCB reduction as KflaHY2 (Figure
459 10) (Hagiwara et al., 2006; DeLano, 2020; Sugishima et al., 2020). The obtained alignments
460 revealed a higher similarity of the KflaHY2 active site to the one of SlHY2. Critical residues of
461 the bottom β-sheet superimpose perfectly, and also the distal Asp residue (SlHY2-
462 Asp^{263}/KflaHY2-Asp^{242}), important for A-ring reduction, is placed similarly (Figure 10A). In
463 contrast, the corresponding residue in SynPcyA (Asp^{220}) is facing outside of the active site and
464 was proven to be not involved in catalysis (Figure 10B) (Hagiwara et al., 2006). On the other
465 hand, the reduction of the D-ring exo-vinyl group in SynPcyA was proven to be catalyzed by
466 the residue Glu^{76}, which does not find a homolog in KflaHY2 (Hagiwara et al., 2006). Based
467 on our biochemical data, Asp^{122} in KflaHY2 could fulfill this function.

468 The specificity of reduction is furthermore influenced by the substrate binding mode of BV,
469 shown to be flipped in the PebB/HY2 lineage of FDBRs (Sommerkamp et al., 2019; Sugishima
470 et al., 2020). We propose this is also true for KflaHY2 as two critical amino acid residues
471 responsible for the stabilization of BV in the *ZZZssa* flipped binding mode are conserved.
472 Overall, the data indicate that the ability of KflaHY2 to synthesize PCB has evolved
473 independently from the biosynthesis catalyzed by PcyA.
474

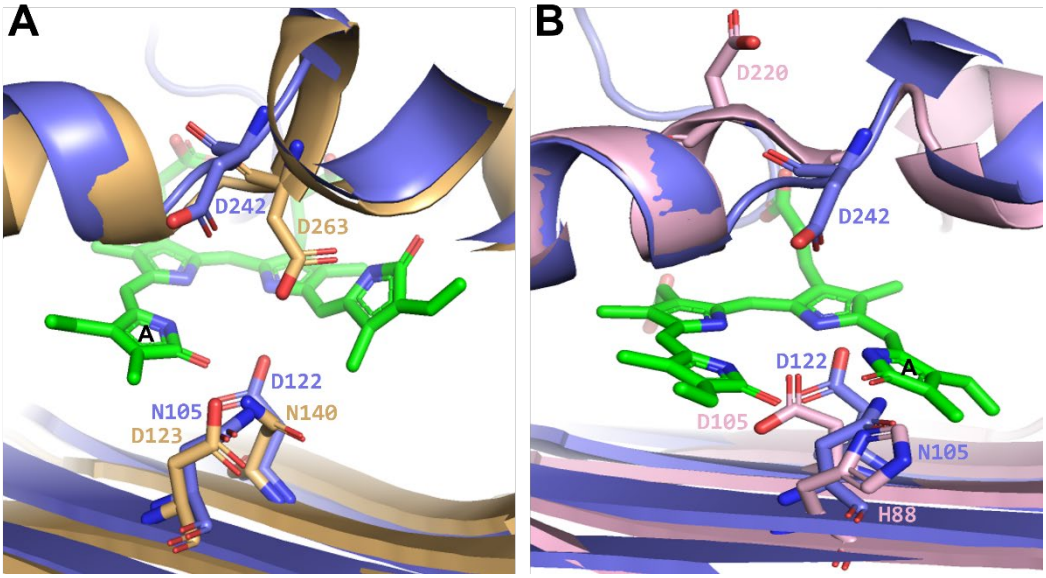

475

476 **Figure 10** Structures alignment of KflaHY2 with SlHY2 and SynPcyA. The model structure of KflaHY2 (displayed
477 in slate cartoon) was obtained using AlphaFold. The alignments were generated using PyMOL (DeLano, 2020). A.
478 Overlay of the active sites of KflaHY2 and SlHY2. The crystal structure of SlHY2 (PDB accession code: 6KME) is
479 displayed as gold cartoon. Biliverdin IXα, in the conformation assumed in the active site of SlHY2, is shown in green,
480 with A-ring being labeled. Amino acid residues of interest are shown as labeled sticks and colored as the belonging
481 structure. B. Overlay of the active sites of KflaHY2 and SynPcyA. The crystal structure of SynPcyA (PDB accession
482 code: 2D1E) is displayed as pink cartoon. Biliverdin IXα, in the conformation assumed in the active site of SlHY2,
483 is shown in green, with A-ring being labeled. Amino acid residues of interest are shown as labeled sticks and colored
484 as the belonging structure.
485
486
487 Surprisingly, our attempt to convert KflaHY2 into a land plant HY2 by exchanging the catalytic
488 pair was unsuccessful in yielding PΦB. We rather revealed that an additional proton donating
489 residue on the β-sheet of the active site induced isomerization of the product to PEB (Figure
490 S3). Product specificity in the HY2 lineage therefore could rather be determined by the
491 architecture of the active site and other residues in the surroundings of the binding pocket.
492 This became even clearer when studying the FDBRs from *Netrium digitus* and *Ceratodon*
493 *purpureus*. Both FDBRs share with KflaHY2 about 48% sequence identity and the same
494 catalytic pair. While the HY2s of *N. digitus* and *K. nitens* are PCB-HY2s and group well with
495 the other characterized HY2 from *Mesotaenium caldariorum* in the phylogenetic tree, the *C.*
496 *purpureus* enzyme is a PΦB-HY2 and forms a monophyletic group with the *Physcomitrella*
497 *patens* HY2 and land plant HY2s (Figure 9). Based on this, we propose that within the HY2
498 lineage, two monophyletic groups diverged from the common HY2 ancestor: the PCB-HY2

499 clade and the PΦB-HY2 clade. Putting these data into perspective, one would therefore
500 suggest that phytochromes with a PΦB chromophore were first found in the bryophytes and
501 that early diverging streptophyte like *Klebsormidium* still possessed a PCB-containing
502 phytochrome. This might be related to the available wavelength of light to these organisms, as
503 a PCB-containing phytochrome will absorb more in the red/orange region of the visible
504 spectrum compared to that a PΦB-containing phytochrome. While these phytochromes are
505 thought to have a common cyanobacterial ancestor, the corresponding FDBR sequences have
506 significantly diversified since primary endosymbiosis (Rockwell and Lagarias, 2017).

Acknowledgement

This project was financially supported by a grant from the Deutsche Forschungsgemeinschaft to NFD and EH. FZ and EH acknowledge support by the Deutsche Forschungsgemeinschaft within the Research Training Group GRK2341 “MiCon”. We furthermore thank J. Clark Lagarias for the gift of plasmids and helpful discussions with him and Nathan Rockwell.

Author contributions

FF, BL and NFD designed research, FF, BL, JH, ZF performed research, EPP and EH contributed analytical tools, FF, BL and NFD wrote the paper. All authors read and approved the final version of the manuscript.

Conflict of Interest

The authors declare no conflict of interest.

522 # References

523 **Busch AWU, Reijerse EJ, Lubitz W, Hofmann E, Frankenberg-Dinkel N** (2011) Radical
524 mechanism of cyanophage phycoerythrobilin synthase (PebS). Biochem. J. doi:
525 10.1042/BJ20101642

526 **Caignan GA, Deshmukh R, Wilks A, Zeng Y, Huang H wei, Moënne-Loccoz P, Bunce RA,**
527 **Eastman MA, Rivera M** (2002) Oxidation of heme to β- and δ-biliverdin by *Pseudomonas*
528 *aeruginosa* heme oxygenase as a consequence of an unusual seating of the heme. J.
529 Am. Chem. Soc. doi: 10.1021/ja0274960

530 **Chen YR, Su YS, Tu SL** (2012) Distinct phytochrome actions in nonvascular plants revealed
531 by targeted inactivation of phytobilin biosynthesis. Proc. Natl. Acad. Sci. USA. doi:
532 10.1073/pnas.1201744109

533 **Cornejo J, Beale SI** (1988) Algal heme oxygenase from *Cyanidium caldarium*. Partial
534 purification and fractionation into three required protein components. J. Biol. Chem. doi:
535 10.1016/s0021-9258(18)37873-6

536 **Dammeyer T, Bagby SC, Sullivan MB, Chisholm SW, Frankenberg-Dinkel N** (2008)
537 Efficient Phage-Mediated Pigment Biosynthesis in Oceanic Cyanobacteria. Curr. Biology.
538 doi: 10.1016/j.cub.2008.02.067

539 **DeLano WL** (2020) The PyMOL Molecular Graphics System, Version 2.3. Schrödinger LLC

540 **Fiege K, Frankenberg-Dinkel N** (2020) Construction of a new T7 promoter compatible
541 *Escherichia coli* Nissle 1917 strain for recombinant production of heme-dependent
542 proteins. Microb. Cell Factories. doi: 10.1186/s12934-020-01447-5

543 **Frankenberg N, Lagarias JC** (2003) Phycocyanobilin:ferredoxin oxidoreductase of *Anabaena*
544 sp. PCC 7120: Biochemical and spectroscopic characterization. J. Biol. Chem. doi:
545 10.1074/jbc.M211643200

546 **Frankenberg N, Mukougawa K, Kohchi T, Lagarias JC** (2001) Functional genomic analysis
547 of the HY2 family of ferredoxin-dependent bilin reductases from oxygenic photosynthetic
548 organisms. Plant Cell. doi: 10.1105/tpc.13.4.965

549 **Gill SC, von Hippel PH** (1989) Calculation of protein extinction coefficients from amino acid
550 sequence data. Anal. Biochem. doi: 10.1016/0003-2697(89)90602-7

551 **Guindon S, Dufayard JF, Lefort V, Anisimova M, Hordijk W, Gascuel O** (2010) New
552 algorithms and methods to estimate maximum-likelihood phylogenies: Assessing the
553 performance of PhyML 3.0. Syst. Biol. doi: 10.1093/sysbio/syq010

554 **Hagiwara Y, Sugishima M, Khawn H, Kinoshita H, Inomata K, Shang L, Lagarias JC,**
555 **Takahashi Y, Fukuyama K** (2010) Structural insights into vinyl reduction regiospecificity
556 of phycocyanobilin:Ferredoxin oxidoreductase (PcyA). J. Biol. Chem. doi:
557 10.1074/jbc.M109.055632

558 **Hagiwara Y, Sugishima M, Takahashi Y, Fukuyama K** (2006) Crystal structure of
559 phycocyanobilin:ferredoxin oxidoreductase in complex with biliverdin IXα, a key enzyme
560 in the biosynthesis of phycocyanobilin. Proc. Natl. Acad. Sci. USA. doi:
561 10.1073/pnas.0507266103
562 **Jumper J, Evans R, Pritzel A, Green T, Figurnov M, Ronneberger O, Tunyasuvunakool**
563 **K, Bates R, Žídek A, Potapenko A, et al** (2021) Highly accurate protein structure
564 prediction with AlphaFold. Nature. doi: 10.1038/s41586-021-03819-2
565 **Kohchi T, Mukougawa K, Frankenberg N, Masuda M, Yokota A, Lagarias JC** (2001) The
566 *Arabidopsis* HY2 gene encodes phytochromobilin synthase, a ferredoxin-dependent
567 biliverdin reductase. Plant Cell. doi: 10.1105/tpc.13.2.425
568 **Lamparter T, Podlowski S, Mittmann F, Schneider-Poetsch H, Hartmann E, Hughes J**
569 (1995) Phytochrome from Protonemal Tissue of the Moss *Ceratodon purpureus*. J. Plant
570 Physiol. doi: 10.1016/S0176-1617(11)82178-4
571 **Ledermann B, Béjà O, Frankenberg-Dinkel N** (2016) New biosynthetic pathway for pink
572 pigments from uncultured oceanic viruses. Environ. Microbiol. doi: 10.1111/1462-
573 2920.13290
574 **Ledermann B, Schwan M, Sommerkamp JA, Hofmann E, Béjà O, Frankenberg-Dinkel N**
575 (2018) Evolution and molecular mechanism of four-electron reducing ferredoxin-
576 dependent bilin reductases from oceanic phages. FEBS J. doi: 10.1111/febs.14341
577 **Lemoine F, Domelevo Entfellner JB, Wilkinson E, Correia D, Dávila Felipe M, De Oliveira**
578 **T, Gascuel O** (2018) Renewing Felsenstein's phylogenetic bootstrap in the era of big
579 data. Nature. doi: 10.1038/s41586-018-0043-0
580 **Letunic I, Bork P** (2021) Interactive tree of life (iTOL) v5: An online tool for phylogenetic tree
581 display and annotation. Nucleic Acids Res. doi: 10.1093/nar/gkab301
582 **Li L, Lagarias JC** (1992) Phytochrome assembly. Defining chromophore structural
583 requirements for covalent attachment and photoreversibility. J. Biol. Chem. doi:
584 10.1016/s0021-9258(18)41762-0
585 **McDowell MT, Lagarias JC** (2001) Purification and biochemical properties of
586 phytochromobilin synthase from etiolated oat seedlings. Plant Physiol. doi:
587 10.1104/pp.126.4.1546
588 **Mirdita M, Schütze K, Moriwaki Y, Heo L, Ovchinnikov S, Steinegger M** (2022) ColabFold:
589 making protein folding accessible to all. Nat. Methods. doi: 10.1038/s41592-022-01488-
590 1
591 **Möglich A, Yang X, Ayers RA, Moffat K** (2010) Structure and function of plant
592 photoreceptors. Annu. Rev. Plant Biol. doi: 10.1146/annurev-arplant-042809-112259
593 **Murphy JT, Lagarias JC** (1997) The phytofluors: A new class of fluorescent protein probes.
594 Curr. Biology. doi: 10.1016/S0960-9822(06)00375-7

595 **Overkamp KE, Gasper R, Kock K, Herrmann C, Hofmann E, Frankenberg-Dinkel N** (2014)
596 Insights into the biosynthesis and assembly of cryptophycean phycobiliproteins. J. Biol.
597 Chem. doi: 10.1074/jbc.M114.591131
598 **Rockwell NC, Lagarias JC** (2017) Ferredoxin-dependent bilin reductases in eukaryotic algae:
599 Ubiquity and diversity. J. Plant Physiol. doi: 10.1016/j.jplph.2017.05.022
600 **Rockwell NC, Martin SS, Li FW, Mathews S, Lagarias JC** (2017) The phycocyanobilin
601 chromophore of streptophyte algal phytochromes is synthesized by HY2. New Phytol. doi:
602 10.1111/nph.14422
603 **Sharrock RA** (2008) The phytochrome red/far-red photoreceptor superfamily. Genome Biol.
604 doi: 10.1186/gb-2008-9-8-230
605 **Sommerkamp JA, Frankenberg-Dinkel N, Hofmann E** (2019) Crystal structure of the first
606 eukaryotic bilin reductase GtPEBB reveals a flipped binding mode of dihydrobiliverdin. J.
607 Biol. Chem. doi: 10.1074/jbc.RA119.009306
608 **Sugishima M, Wada K, Fukuyama K, Yamamoto K** (2020) Crystal structure of
609 phytochromobilin synthase in complex with biliverdin IXα, a key enzyme in the
610 biosynthesis of phytochrome. J. Biol. Chem. doi: 10.1074/jbc.RA119.011431
611 **Tasler R, Moises T, Frankenberg-Dinkel N** (2005a) Biochemical and spectroscopic
612 characterization of the bacterial phytochrome of *Pseudomonas aeruginosa*. FEBS J. doi:
613 10.1111/j.1742-4658.2005.04623.x
614 **Tu SL, Chen HC, Ku LW** (2008) Mechanistic studies of the phytochromobilin synthase HY2
615 from *Arabidopsis*. J. Biol. Chem. doi: 10.1074/jbc.M803761200
616 **Tu SL, Gunn A, Toney MD, Britt RD, Lagarias JC** (2004) Biliverdin reduction by
617 cyanobacterial phycocyanobilin:ferredoxin oxidoreductase (PcyA) proceeds via linear
618 tetrapyrrole radical intermediates. J. Am. Chem. Soc. doi: 10.1021/ja049280z
619 **Wu SH, McDowell MT, Lagarias JC** (1997) Phycocyanobilin is the natural precursor of the
620 phytochrome chromophore in the green alga *Mesotaenium caldariorum*. J. Biol. Chem.
621 doi: 10.1074/jbc.272.41.25700
622 **Xu QZ, Bielytskyi P, Otis J, Lang C, Hughes J, Zhao KH, Losi A, Gärtner W, Song C**
623 (2019) MAS NMR on a red/far-red photochromic cyanobacteriochrome All2699 from
624 *Nostoc*. Int. J. Mol. Sci. doi: 10.3390/ijms20153656
625

Figure legends

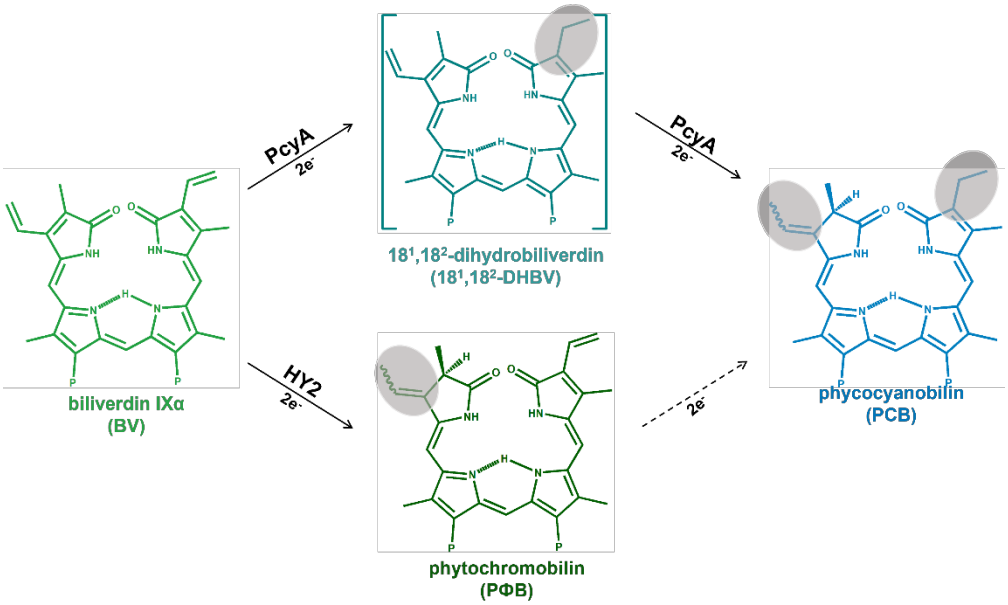

Figure 2 Overview of the reactions catalyzed by the FDBRs HY2 and PcyA. BV is the substrate of the FDBRs in question. “P” indicates the propionate side chains. Land Plants HY2 catalyzes the two-electron reduction of BV to PΦB. PcyA catalyzes the four-electron reduction of BV to PCB via the intermediate $18^1,18^2$-DHBV. Dashed line represents a possible second pathway to PCB.

633

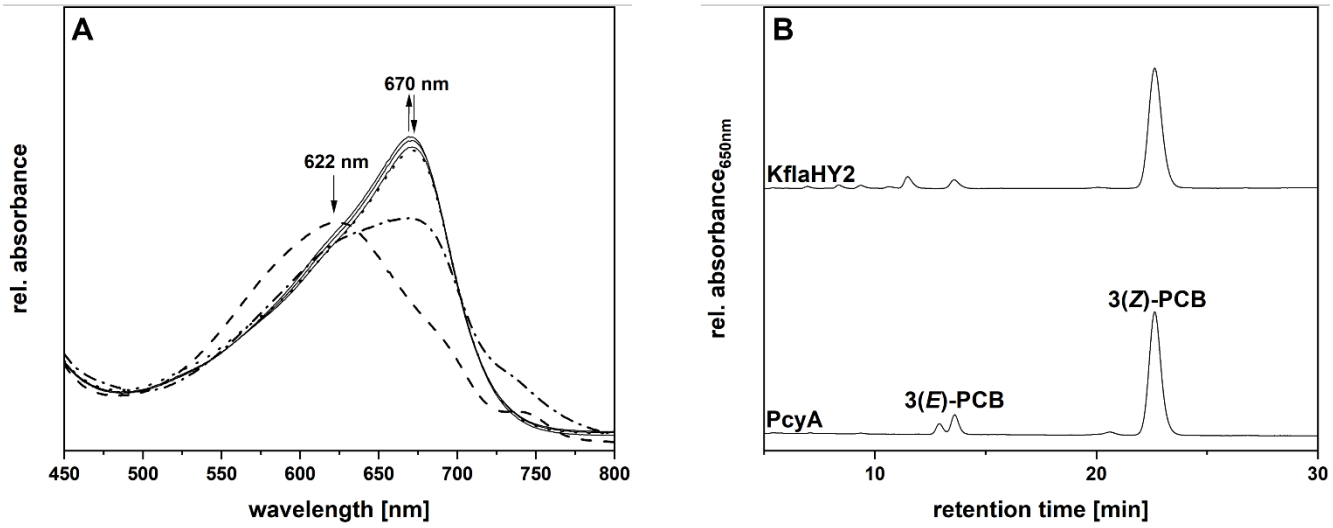

634

635 **Figure 2** Activity assay of recombinant KflaHY2 employing BV as the substrate and characterization of reaction
636 products. A. Time-resolved UV-Vis spectra of an anaerobic bilin reductase activity of recombinant KflaHY2
637 employing BV as the substrate. Total reaction time was 5 min and spectra were recorded every 30s. The course of
638 the spectra is marked by arrows. For reasons of clarity, only relevant spectra are shown. The dashed spectrum was
639 acquired without starting the reaction. The dotted-dashed spectrum represents the first acquired after starting the
640 reaction. The dotted curve represents the end spectrum. B. HPLC analyses of the reaction products of KflaHY2
641 with BV as substrate. The products were analyzed using a reversed-phase 5 µm C18 Luna column (Phenomenex)
642 as stationary phase. The mobile phase consisted of 50% (v/v) acetone and 50% (v/v) 20 mM formic acid flowing at
643 0.6 mL/min. Products of an anaerobic turnover of BV to PCB mediated by PcyA served as standards. Absorbance
644 was continuously recorded at 650 nm.

645

646

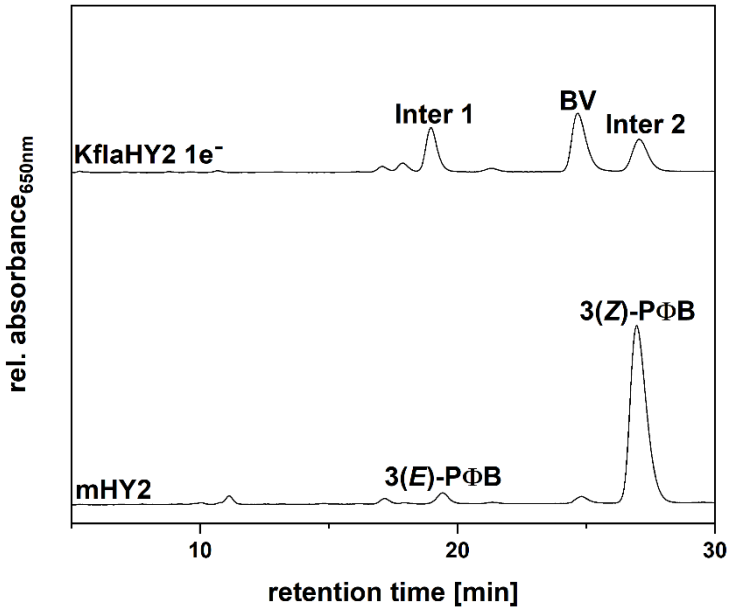

647

648 **Figure 3** HPLC analyses of the reaction products of an anaerobic activity assay employing equimolar amounts of
649 KflaHY2 and BV with one electron equivalent of NADPH. Products were resolved using a reversed-phase 5 µm
650 C18 Luna column (Phenomenex) as stationary phase and a mixture of 50% (v/v) acetone and 50% (v/v) 20 mM
651 formic acid as mobile phase at 0.6 mL/min. The products of an anaerobic turnover of BV to PΦB mediated by HY2
652 derived from *A. thaliana* were used as standards. Absorbance was continuously recorded at 650 nm.

653

654

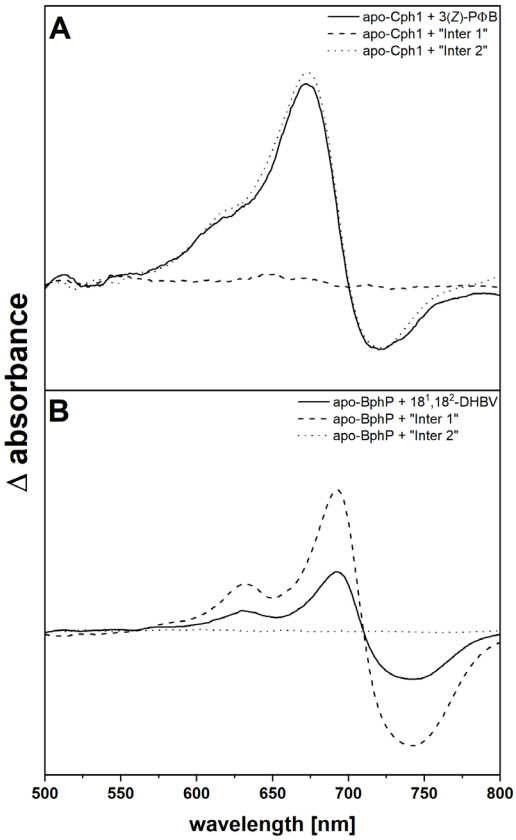

655

656 **Figure 4** Red/far-red light induced difference spectra of coupled phytochrome assembly assays employing the
657 intermediates of the KflaHY2 reaction. Absorbance spectra were recorded after incubation for 3 min with red light
658 (636 nm – Pfr spectrum) and after incubation for 3 min with far red light (730 nm for Cph1; 750 nm for BphP – Pr
659 spectrum). Difference spectra were calculated by the subtraction of the Pfr from the Pr spectrum. All calculated
660 difference spectra were smoothed applying a 20 pt. Savitzky-Golay filter. A. Coupled phytochrome assembly assays
661 employing apo-Cph1 and "Inter 1" (dashed line); apo-Cph1 and "Inter 2" (dotted line); apo-Cph1 and 3(*Z*)-PΦB
662 (solid line) B. Coupled phytochrome assembly assay employing apo-BphP and "Inter 1" (dashed line); apo-BphP
663 and "Inter 2" (dotted line); apo-BphP and 18^1,18^2-DHBV (solid line).

664

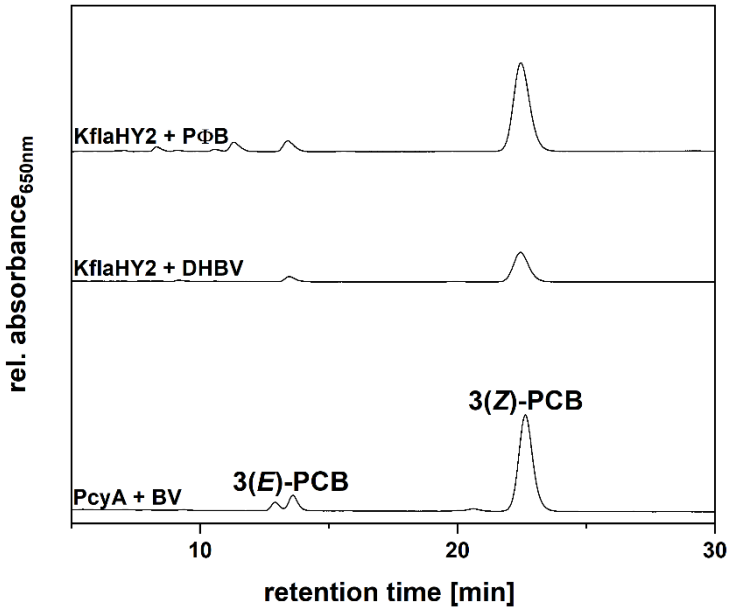

Figure 5 HPLC analyses of the reaction products of activity tests employing 3(*Z*)-PΦB and 18^1,18^2-DHBV as substrates for KflaHY2. Products were analyzed using a 5 µm reversed-phase C18 Luna column (Phenomenex) as stationary phase. The mobile phase consisted of 50% (v/v) acetone and 50% (v/v) 20 mM formic acid flowing at 0.6 mL/min. Reaction products of a PcyA mediated reduction of BV to PCB were used as standards. Absorbance was continuously measured at 650 nm.

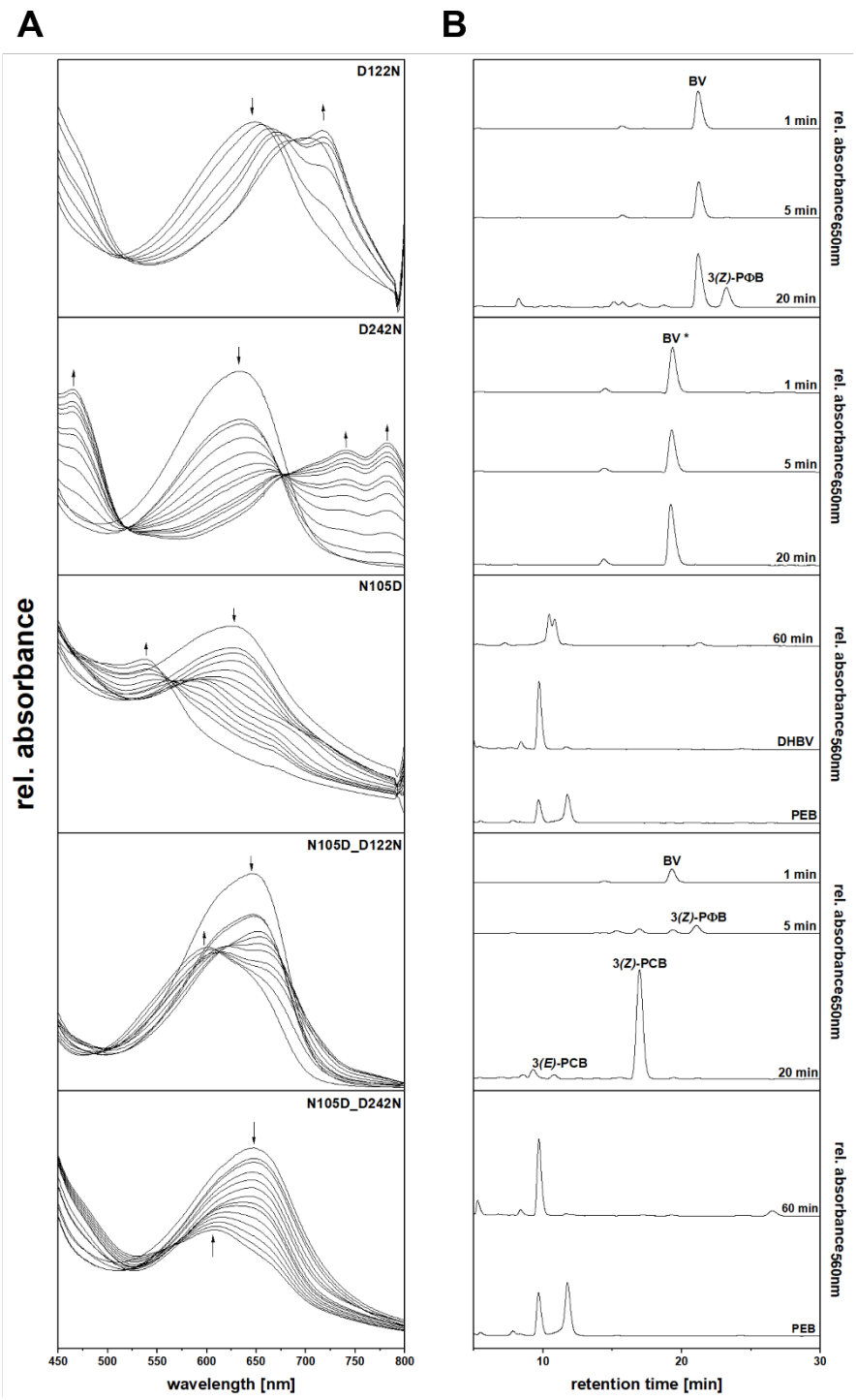

Figure 6 Activity assay and characterization of reaction products of recombinant KflaHY2 variants. A. UV-Vis spectra of the anaerobic FDBR Assay performed using KflaHY2 variants and BV as the substrate. Total reaction time was 20 minutes for KflaHY2_D122N, KflaHY2_D242N, KflaHY2_N105D_D122N and 60 min for KflaHY2_N105D, KflaHY2_N105D_D242N. Spectra were recorded every 30 seconds. For reasons of clarity, only relevant spectra are shown. The arrow indicates the course of absorbance during the reaction. B. HPLC elution profiles of the reaction products of KflaHY2 variants. The stationary phase consisted in a Luna 5µm reversed phase C18 column (Phenomenex). The mobile phase consisted of a mixture of 50% (v/v) acetone and 50% (v/v) 20mM formic acid flowing at 0.6 mL/min. Absorbance was continuously recorded at 560 or 650 nm. BV shows change in the retention time due to substitution of the mobile phase between the different HPLC measurements (*).

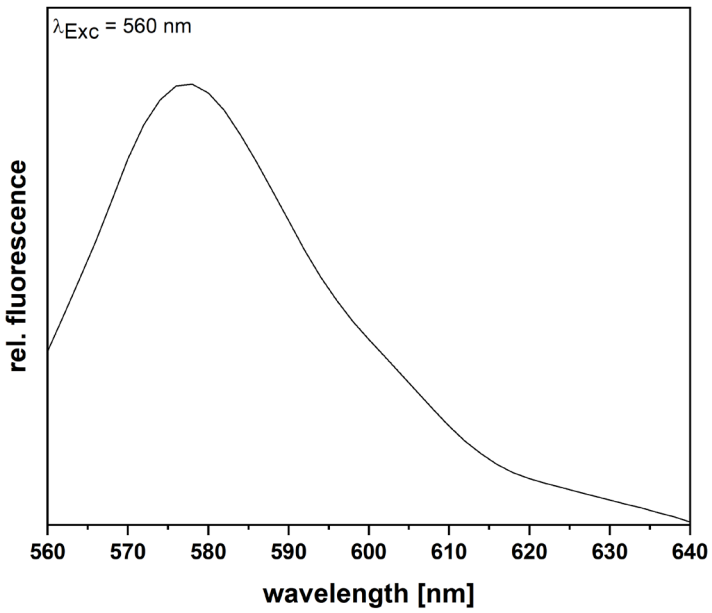

682

683 **Figure 7** Fluorescence emission spectrum of the apo-Cph1-KflaHY2_N105D reaction product adduct. The isolated
684 bilin produced by KflaHY2_N105D was incubated for 30 min in the dark with the lysate of a pET_*cph1*
685 overproduction. Fluorescence emission was recorded after excitation at 560 nm.
686

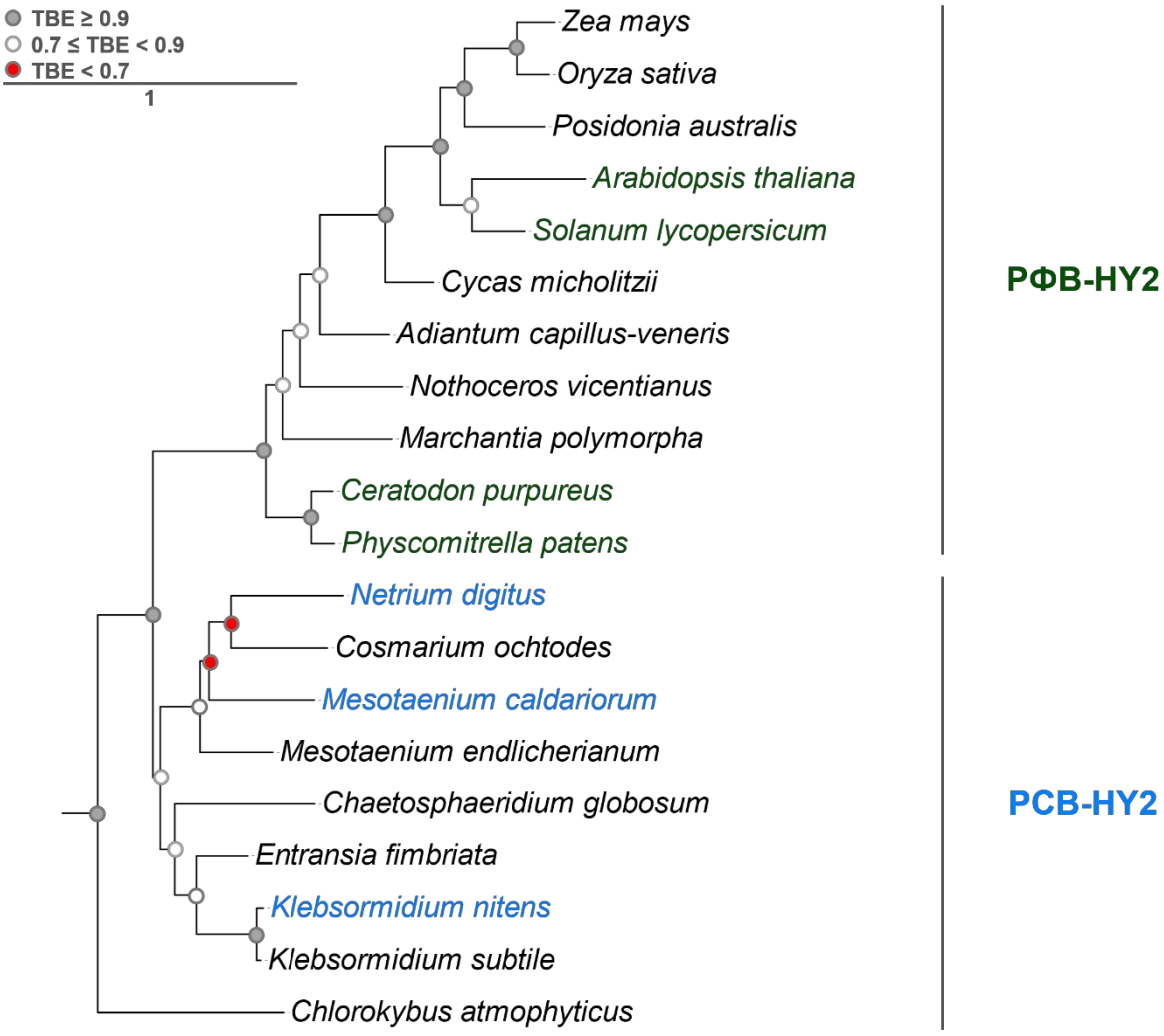

Figure 8 Phylogenetic analysis of HY2 lineage. The maximum-likelihood tree was inferred using PhyML (Guindon et al., 2010). Transfer bootstrap expectation (TBE) was used for support. The represented tree is an excerpt of a full tree including members of all the FDBRs lineages (Figure S). Accession numbers of the employed sequences shown in this figure are available in Supplement material (Table S3). Labels indicate HY2-belonging organism. The color of the label represents the produced bilin (cyan for PCB, dark green for PΦB). Only HY2 with experimentally proven activity are colored. Circles at nodes indicate TBE (grey, TBE ≥ 0.9; white, 0.7 ≤ TBE < 0.9; red, TBE < 0.7).

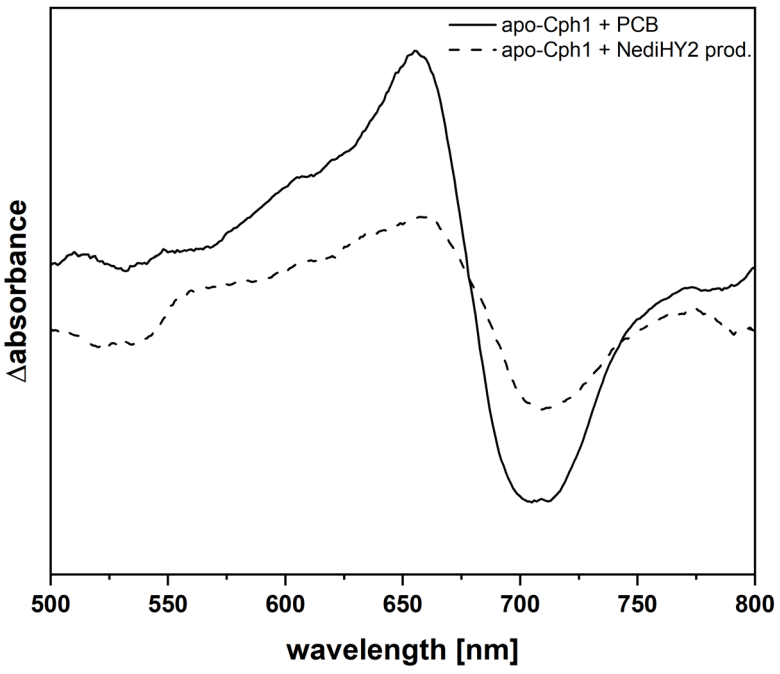

Figure 9 Red/far-red light induced difference spectra of coupled phytochrome assembly assays employing PCB and the product of the NediHY2 reaction. Absorbance spectra were recorded after incubation for 3 min with red light (636 nm – Pfr spectrum) and after incubation for 3 min with far red light (730 nm – Pr spectrum). Difference spectra were calculated by the subtraction of the Pfr from the Pr spectrum. The apo-Cph1 + PCB difference spectrum (solid line) was smoothed applying a 20 pt. Savitzy-Golay filter. The apo-Cph1 + NediHY2 prod. difference spectrum (dashed line) was smoothed applying a 80 pt. Savitzky-Golay filter.

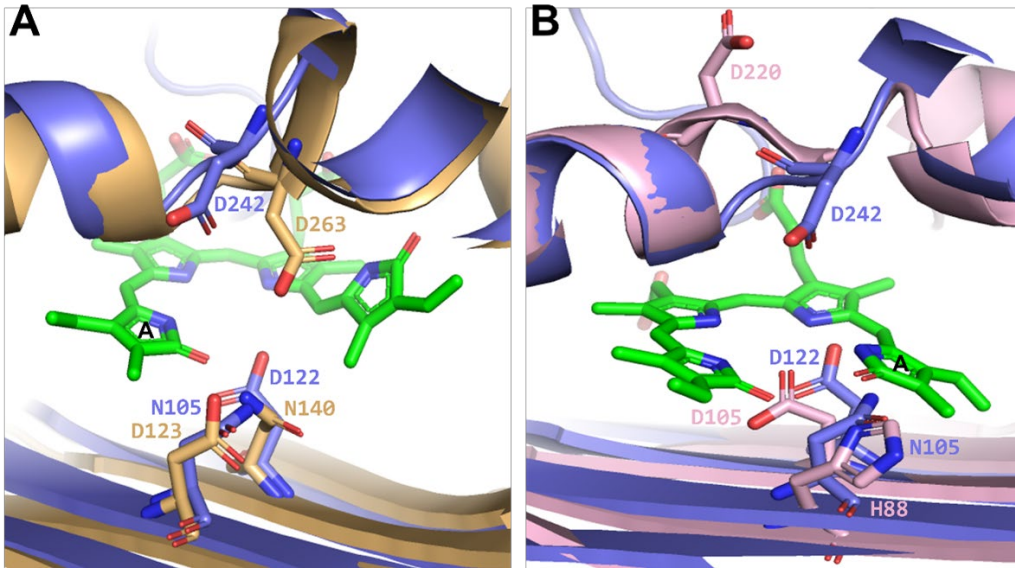

Figure 10 Structures alignment of KflaHY2 with SlHY2 and SynPcyA. The model structure of KflaHY2 (displayed in slate cartoon) was obtained using AlphaFold. The alignments were generated using PyMOL (DeLano, 2020). A. Overlay of the active sites of KflaHY2 and SlHY2. The crystal structure of SlHY2 (PDB accession code: 6KME) is displayed as gold cartoon. Biliverdin IXα, in the conformation assumed in the active site of SlHY2, is shown in green, with A-ring being labeled. Amino acid residues of interest are shown as labeled sticks and colored as the belonging structure. B. Overlay of the active sites of KflaHY2 and SynPcyA. The crystal structure of SynPcyA (PDB accession code: 2D1E) is displayed as pink cartoon. Biliverdin IXα, in the conformation assumed in the active site of SlHY2, is shown in green, with A-ring being labeled. Amino acid residues of interest are shown as labeled sticks and colored as the belonging structure.